

See discussions, stats, and author profiles for this publication at: <https://www.researchgate.net/publication/231538079>

Moore MC, Mills MM, Achterberg EP, Geider RJ, LaRoche J, Lucas MI et al.. Large-scale distribution of Atlantic nitrogen fixation controlled by iron availability. Nat Geosci 2: 867-...

Article in Nature Geoscience · November 2009

Impact Factor: 11.74 · DOI: 10.1038/NGE0667

CITATIONS

166

READS

96

13 authors, including:



[Richard J. Geider](#)

University of Essex

162 PUBLICATIONS 10,545 CITATIONS

[SEE PROFILE](#)



[Alex J Poulton](#)

National Oceanography Centre

84 PUBLICATIONS 1,967 CITATIONS

[SEE PROFILE](#)



[Micha J A Rijkenberg](#)

NIOZ Royal Netherlands Institute for Sea R...

67 PUBLICATIONS 1,204 CITATIONS

[SEE PROFILE](#)

Large-scale distribution of Atlantic nitrogen fixation controlled by iron availability

C. Mark Moore^{1,2*}, Matthew M. Mills³, Eric P. Achterberg², Richard J. Geider¹, Julie LaRoche⁴, Mike I. Lucas⁵, Elaine L. McDonagh², Xi Pan², Alex J. Poulton², Micha J. A. Rijkenberg², David J. Suggett¹, Simon J. Ussher⁶ and E. Malcolm S. Woodward⁷

Oceanic fixed-nitrogen concentrations are controlled by the balance between nitrogen fixation and denitrification¹⁻⁴. A number of factors, including iron limitation⁵⁻⁷, can restrict nitrogen fixation, introducing the potential for decoupling of nitrogen inputs and losses^{2,5,8}. Such decoupling could significantly affect the oceanic fixed-nitrogen inventory and consequently the biological component of ocean carbon storage and hence air-sea partitioning of carbon dioxide^{2,5,8,9}. However, the extent to which nutrients limit nitrogen fixation in the global ocean is uncertain. Here, we examined rates of nitrogen fixation and nutrient concentrations in the surface waters of the Atlantic Ocean along a north-south 10,000 km transect during October and November 2005. We show that rates of nitrogen fixation were markedly higher in the North Atlantic compared with the South Atlantic Ocean. Across the two basins, nitrogen fixation was positively correlated with dissolved iron and negatively correlated with dissolved phosphorus concentrations. We conclude that inter-basin differences in nitrogen fixation are controlled by iron supply rather than phosphorus availability. Analysis of the nutrient content of deep waters suggests that the fixed nitrogen enters North Atlantic Deep Water. Our study thus supports the suggestion that iron significantly influences nitrogen fixation⁵, and that subsequent interactions with ocean circulation patterns contribute to the decoupling of nitrogen fixation and loss^{2,4,8}.

The production and remineralization of organic material in the ocean typically results in a nitrogen (N) to phosphorus (P) ratio ($r_{n/p}$) of $\sim 16:1$ (refs 1, 3, 4, 10). However, the net influences of dinitrogen (N_2) fixation and fixed-nitrogen loss by denitrification and/or anaerobic ammonium oxidation (anammox), generate deviations of the dissolved N/P ratio away from this typical value^{2,4,11}. Removal of NO_3^- in sediments and suboxic water-column oxygen-minimum zones (OMZs) reduces the availability of fixed-N relative to P. An excess of P is thus generated, which may subsequently favour diazotrophic growth and hence ultimately replacement of the lost N (refs 1, 3, 4). This feedback mechanism probably maintains the marine N inventory and couples it to the P inventory^{3,4,12}, at least on long timescales². However, diazotrophic growth may be limited by factors other than the availability of excess P (refs 2, 5, 8, 13). For example, the apparent dominance of oceanic N_2 fixation by facultative diazotrophic cyanobacteria^{7,14} seems to constrain

high rates to well-lit N-limited surface waters^{6,13}. Furthermore, iron (Fe) limitation of diazotrophs⁵⁻⁷ may further contribute to decoupling of N inputs and losses, generating the potential for perturbations in the N inventory as a result of past or future climate change^{2,5,8,9,15}. Although limited correlative evidence supports the Fe-limitation hypothesis¹⁶⁻¹⁸, direct experimental tests are rare⁶. Moreover, recent interpretation of nutrient distributions calls for tight spatial coupling of N_2 fixation and denitrification, suggesting that the N/P feedback mechanism operates efficiently in the modern ocean, potentially implying a limited role for Fe limitation⁴.

On a meridional transect between 37° N and 35° S in the Atlantic Ocean (Fig. 1), we observed maximum surface and euphotic-zone integrated N_2 fixation rates north of the Equator (Fig. 2a,b, Supplementary Fig. S1a). N_2 fixation by unicellular ($<20\ \mu\text{m}$) diazotrophs contributed a background of $16 \pm 7\ \mu\text{mol N m}^{-2}\ \text{d}^{-1}$ throughout the transect, whereas N_2 fixation by the larger size fraction, dominated by the diazotrophic filamentous cyanobacteria *Trichodesmium* spp. (Fig. 2c), peaked between ~ 5 and 15° N at $\sim 200\ \mu\text{mol m}^{-2}\ \text{d}^{-1}$. Although diazotroph distributions may vary seasonally^{13,14}, data available at present suggest that the observed inter-hemispheric contrast is broadly persistent¹⁷. In turn, *Trichodesmium* abundance and N_2 fixation rates were both positively correlated with dissolved iron (see Supplementary Table S1) and dissolved aluminium, a non-nutrient tracer of atmospheric dust input (Fig. 2d,e).

Surface concentrations of dissolved inorganic N (DIN) were low throughout the transect and indistinguishable between northern and southern gyres ($5 \pm 3\ \text{nmol l}^{-1}\ \text{NO}_3^- + \text{NO}_2^-$ (Fig. 2f) and $17 \pm 8\ \text{nmol l}^{-1}\ \text{NH}_4^+$). In contrast, dissolved inorganic P (DIP) was over an order of magnitude higher in the surface waters of the southern gyre ($210 \pm 60\ \text{nmol l}^{-1}$) than the potentially biolimiting concentrations ($9 \pm 4\ \text{nmol l}^{-1}$) observed in the northern gyre (Fig. 2f). Dissolved organic P (DOP) concentrations were also significantly lower in the northern sub-tropical gyre ($0.19 \pm 0.02\ \mu\text{mol l}^{-1}$) than in the south ($0.28 \pm 0.02\ \mu\text{mol l}^{-1}$), whereas DON averaged $\sim 6\ \mu\text{mol l}^{-1}$ in both gyres. Excess DIP was calculated as $P^* = \text{DIP} - \text{DIN}/r_{n/p}$. Similarly, the related term $N^* (= -r_{n/p} P^*)$ provides a measure of excess DIN relative to DIP (ref. 11) and $\text{DOP}^* (= \text{DOP} - \text{DON}^*/r_{n/p})$ and $\text{TDP}^* (= P^* + \text{DOP}^*)$ can be used to indicate the excess of the organic and total dissolved P pools respectively. Assuming $r_{n/p} = 16:1$ (refs 1, 10), P^* increased from $<0.016\ \mu\text{mol l}^{-1}$ in the northern gyre to $\sim 0.2\ \mu\text{mol l}^{-1}$ in the

¹Department of Biological Sciences, University of Essex, Colchester CO4 3SQ, UK, ²National Oceanography Centre, University of Southampton, European Way, Southampton SO14 3ZH, UK, ³Department of Environmental Earth System Science, Stanford University, Stanford, California 94305, USA, ⁴Marine Biogeochemistry, Leibniz-Institut für Meereswissenschaften, D-24105 Kiel, Germany, ⁵Department of Zoology, University of Cape Town, Rondebosch 7701, South Africa, ⁶School of Earth, Ocean and Environmental Sciences, University of Plymouth, Plymouth PL4 8AA, UK, ⁷Plymouth Marine Laboratory, Prospect Place, The Hoe, Plymouth PL1 3DH, UK. *e-mail: cmm297@noc.soton.ac.uk.

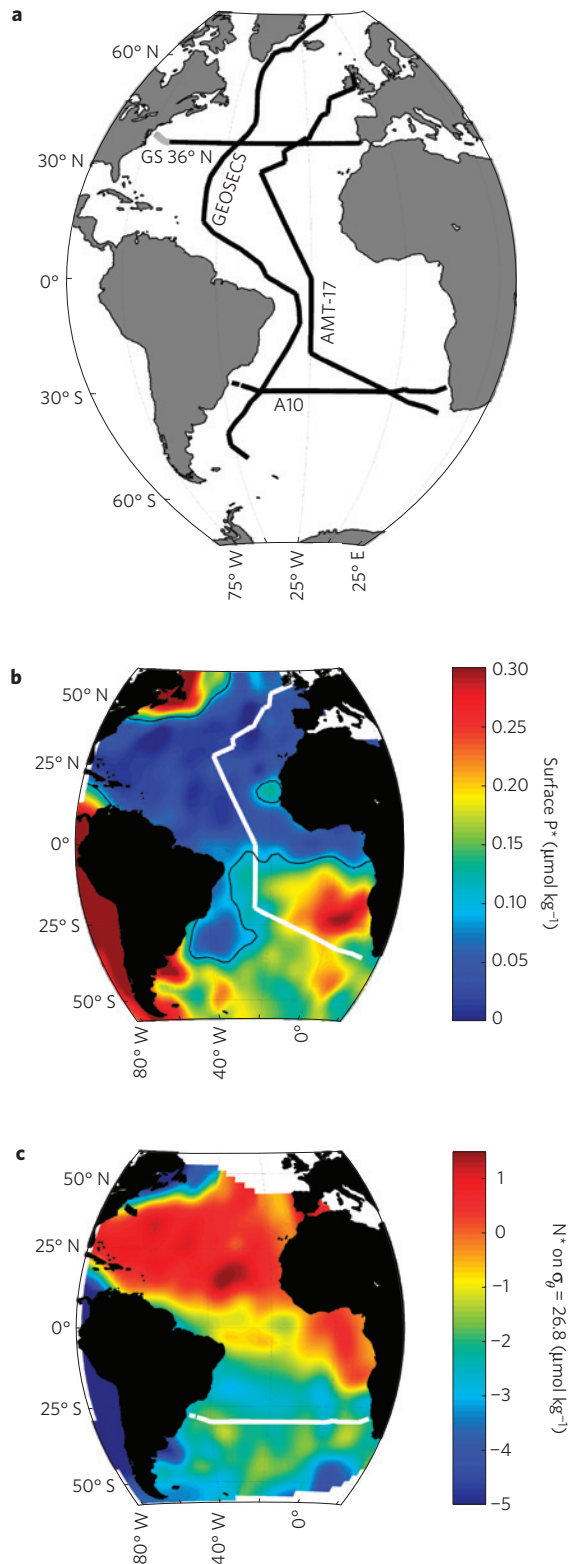


Figure 1 | Cruise tracks and maps of annual mean excess nutrient distributions. **a**, Cruise tracks for the AMT-17 cruise and hydrographic sections (WOCE A10, GEOSECS and the 1981 occupation of 36° N, including the Gulf Stream (GS)) used in the analysis of deep ocean nutrient distributions and transport. **b**, Climatological surface P^* ($= \text{DIP} - \text{DIN}/r_{n/p}$) distribution with the AMT-17 cruise track and a contour corresponding to $0.1 \mu\text{mol kg}^{-1} P^*$ superimposed. **c**, Distribution of N^* ($= -r_{n/p} P^*$) on the $\sigma_\theta = 26.8$ surface corresponding to the thermocline/SAMW (ref. 24) with WOCE A10 (white) and GS 36° N (black) sections indicated.

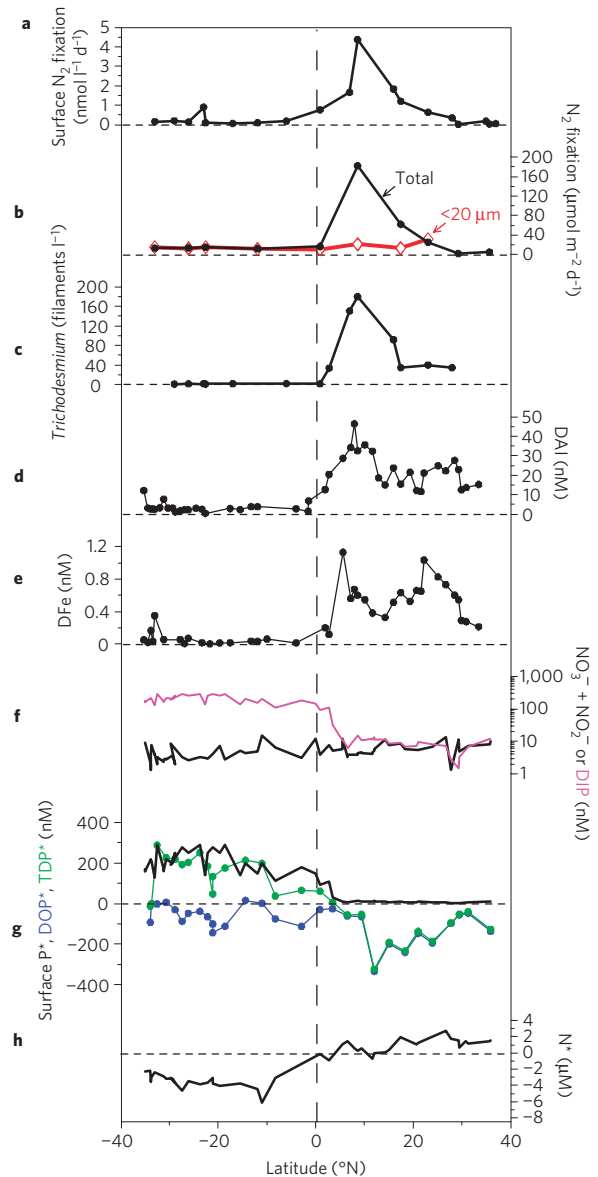


Figure 2 | Transect data from the AMT-17 cruise. **a**, Surface N_2 fixation rate. **b**, Total and $<20 \mu\text{m}$ integrated water-column rates of N_2 fixation. **c**, Surface *Trichodesmium* distribution. **d**, Dissolved aluminium (DAI). **e**, Dissolved iron (DFe). **f**, $\text{NO}_3^- + \text{NO}_2^-$ and DIP (note logarithmic scale). **g**, P^* ($= \text{DIP} - \text{DIN}/r_{n/p}$), DOP^* ($= \text{DOP} - \text{DON}/r_{n/p}$) and TDP^* ($= P^* + \text{DOP}^*$). **h**, N^* ($= \text{DIN} - r_{n/p} \text{DIP}$) at the nutricline, defined as $\text{DIN} = 1 \mu\text{mol l}^{-1}$.

south. Moreover, DOP^* was more negative in the northern gyre (Fig. 2g and Supplementary Fig. S1c). Marked gradients were thus observed in surface TDP^* , with positive values in the southern gyre and negative values in the north (Fig. 2g), which were spatially correlated with the region of enhanced N_2 fixation (Fig. 2, Supplementary Fig. S1).

These data clearly do not support a proximal role for surface-water P availability as a control on the spatial distribution of N_2 fixation across inter-basin scales in the Atlantic. Higher (TD)P and (TD) P^* concentrations observed in the South Atlantic probably result from exchanges with low N/P (negative N^*) thermocline waters (Fig. 2h) as well as lateral transport of N-deficient waters generated in the Benguela current system⁴ (Fig. 1b). The severely N-deficient waters were shown to result in N limitation of bulk community productivity (see Supplementary Fig. S2). Clearly some

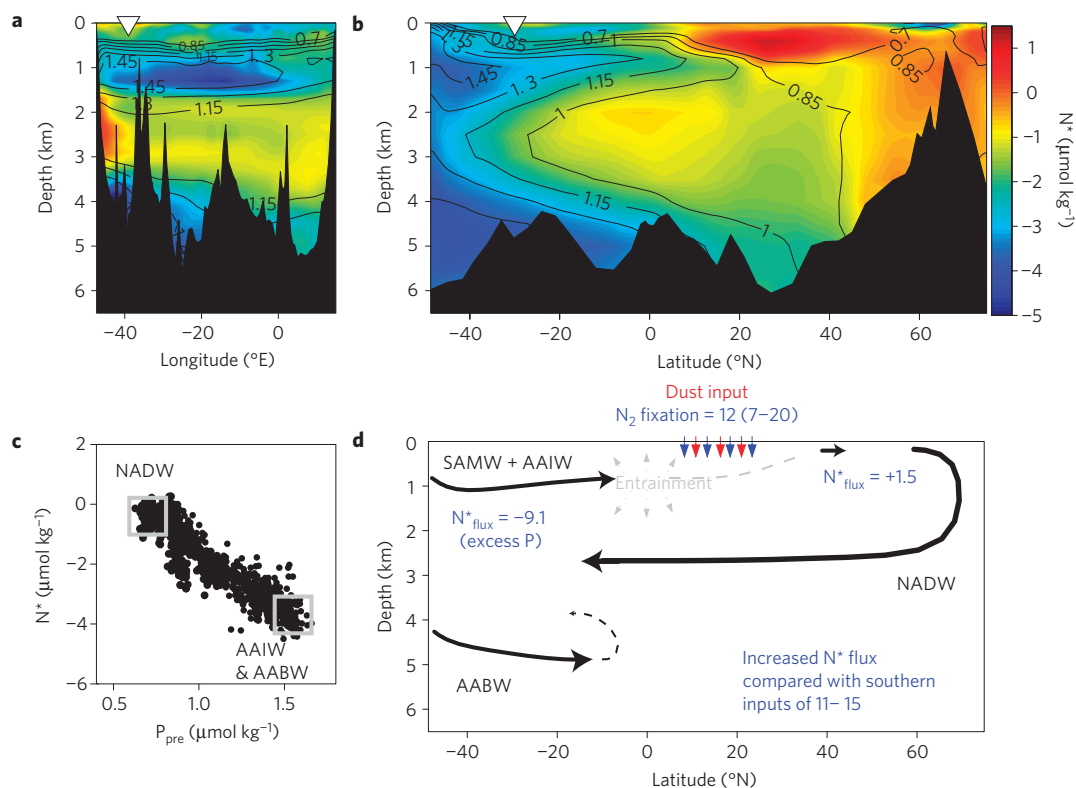


Figure 3 | Deep water N* distribution and fluxes in the Atlantic. **a**, Zonal section of N* (= DIN - r_{n/p} DIP) at 30° S with overlaid contours of preformed phosphate (P_{pre}, μmol kg⁻¹). **b**, GEOSECS meridional section of N* throughout the western Atlantic with overlaid contours of P_{pre}. The triangles indicate crossover points of transects. **c**, Relationship of N* to P_{pre}, a tracer of NADW, in Atlantic waters below 750 m (1,500 m in the north). Endmember concentrations are indicated. **d**, Schematic diagram showing suggested transport pathways and corresponding N fluxes in the Atlantic; all values are in units of 10¹¹ mol N yr⁻¹.

Table 1 | Estimates of N inputs to the open Atlantic Ocean and the global ocean.

Process	Method	Value (10 ¹¹ mol N yr ⁻¹)	Reference
North Atlantic N ₂ fixation	Scaled direct biological rates for <i>Trichodesmium</i>	16	14
	N* accumulation in the thermocline	20	11
	N* accumulation in thermocline*	4 (7)	20
Whole Atlantic N ₂ fixation	P* flux convergence	14	4
Net N* increase in Atlantic overturning circulation	N* divergence in upper limb between 30° S and 36° N [†]	11 ± 3	This study
	Deep water N* distribution combined with NADW formation rate [‡]	15 ± 4	This study
Global N ₂ fixation	P* flux convergence	100	4

Recalculated value in parenthesis assumes that negative values of DOP in surface waters of the North Atlantic ultimately result from the net influence of N₂ fixation (Fig. 2). Remineralization of this material within the thermocline²⁰ should then be included in estimates of N₂ fixation.

[†] See Supplementary Information.

[‡] Difference in N* of 3.3 ± 0.6 (Fig. 3c) multiplied by a NADW formation rate of 15 ± 2 Sv (ref. 29).

factor other than P availability prevents N₂ fixation from fully replacing this fixed-N deficit. Between ~10° S and ~3° N, deeper mixed layers may have contributed to reduced N₂ fixation^{13,17} (see Supplementary Fig. S1). However, for the wider South Atlantic gyre, we suggest that the extremely low Fe concentrations (mean 30 ± 20 pmol l⁻¹) were limiting diazotrophy, in particular for *Trichodesmium* spp.⁷ (Fig. 2).

In contrast, enhanced Fe input from dust deposition to the North Atlantic seems to result in increased diazotrophy^{6,12,16,17}

(Fig. 2). Consequently, surface DIP is drawn down to very low concentrations¹², depleting P* to near zero. Further P required for continued N₂ fixation probably comes from the DOP pool¹⁹ (Fig. 2g, Supplementary Fig. S1), resulting in lower DOP and negative DOP* and TDP*. As previously argued in support of the Fe hypothesis¹¹, the subsequent export of diazotrophically derived organic material with a high N/P ratio results in the accumulation of excess DIN within the thermocline of the northern gyre^{11,12,20} (Fig. 1c). The net removal of P from the surface waters and input of

N to the system as a whole probably contributes to the observed NP co-limitation of the bulk community in the North Atlantic gyre^{6,21} as well as (Fe-)P (co-)limitation of diazotrophy^{6,22}. Consequently, the inter-hemispheric pattern of N₂ fixation in the Atlantic seems to be controlled by Fe input (Fig. 2). Nutrient climatologies for both surface and thermocline waters (Fig. 1b,c) suggest that the resulting gradient in N₂ fixation^{14,17} has a persistent influence on the coupling of N to P at basin scales in the Atlantic.

Although observed high rates of N₂ fixation in the northern gyre¹⁴ may be locally supported by the utilization of DOP (ref. 19, Fig. 2, Supplementary Fig. S1), over larger scales an ultimate source of excess P is required⁴. In contrast to the situation in the Indian and Pacific oceans⁴, the well-ventilated North Atlantic lacks a significant suboxic OMZ and hence the source of excess P is probably non-local. A proportion of the required excess P may be provided by transport through the Arctic²³. However, northward transport and subsequent entrainment of thermocline and intermediate waters originating in the Southern Ocean seems to be the main supply route of nutrients to the Atlantic^{24,25}.

Using calculated volume fluxes²⁶ combined with observed N* distributions on a World Ocean Circulation Experiment (WOCE) section at 30° S (Fig. 3a), we estimate a northward N* flux of $-9.1 \pm 2.5 \times 10^{11} \text{ mol yr}^{-1}$ within thermocline/intermediate Sub-Antarctic Mode Water (SAMW) and Antarctic Intermediate Water (AAIW) (see Supplementary Fig S3 and Table S2). This flux corresponds to an excess P input of $\sim 4\text{--}7 \times 10^{10} \text{ mol yr}^{-1}$, at least twice that transported through the Arctic²³. Export of high N/P organic material into the thermocline¹¹ is probably restricted by Fe limitation of diazotrophy in the South Atlantic (Figs 2 and 1c). Consequently, we suggest that the excess P flux within SAMW and AAIW largely transits under the southern gyre, into the North Atlantic^{24,25} (Figs 2h and 1c), where it would be sufficient to support estimated N₂ fixation rates^{11,14} (Table 1). Reductions in this transport might therefore be expected to decrease diazotrophy in the North Atlantic. Consequently ocean circulation^{15,27} should potentially be considered alongside changes in dust deposition^{5,8,9} as a control on N₂ fixation.

Published volume and nutrient transport data in the Gulf Stream at 36° N (ref. 25) were combined to estimate a northward N* transport of $4.3 \times 10^{11} \text{ mol yr}^{-1}$, most of which will recirculate within the sub-tropical gyre system²⁵. However, we estimate that $1.5 \pm 2 \times 10^{11} \text{ mol N* yr}^{-1}$ will be transported north into the subpolar gyre (see Supplementary Information). Consequently, between 30° S and the subpolar gyre, the upper limb of the Atlantic meridional overturning circulation (AMOC) gains $11 \pm 3 \times 10^{11} \text{ mol N* yr}^{-1}$ (Table 1) (formally a N* flux divergence²⁸), most of which seems to occur north of the Equator (Figs 1c and 3b).

The distribution of N* in deep waters (>1,000 m) was further found to be highly correlated with preformed phosphate (P_{pre}), a good tracer of North Atlantic Deep Water (NADW) (Fig. 3a,b, Supplementary Fig. S4). N* thus behaves conservatively below the thermocline in the Atlantic (Fig. 3c), decreasing from the NADW endmember ($-0.4 \pm 0.4 \mu\text{mol kg}^{-1}$), to values representative of both the deep (Antarctic Bottom Water, AABW) and thermocline/intermediate (SAMW and AAIW) southern endmembers ($-3.7 \pm 0.4 \mu\text{mol kg}^{-1}$). As previously suggested², rates of NADW formation²⁹ can then be used to calculate a N* flux divergence of $15 \pm 4 \times 10^{11} \text{ mol N yr}^{-1}$ between the northern end of the lower (return) limb of the AMOC and southern source waters (Fig. 3b,d). We interpret these estimates of excess N added to water masses during transit of the AMOC as measures of the net rate of N₂ fixation (and other N inputs) over that of fixed-N losses^{2,28} (see also Supplementary Information). Net excess N inputs seem to be of comparable magnitude to current biological and most geochemical estimates of N₂ fixation in the North Atlantic (Table 1). Our analysis

thus suggests that most of the N input resulting from N₂ fixation in the North Atlantic enters the deep oceanic circulation (Fig. 3d), as might be expected given the lack of a suboxic OMZ and hence water-column fixed-N loss in this basin².

High rates of N₂ fixation probably resulting from Fe supply to the North Atlantic (Fig. 2), coupled with the lack of major fixed-N loss², therefore seem to result in an $\sim 3 \mu\text{mol kg}^{-1}$ increase of N* within NADW. The increased N exported within NADW, which contributes half the global formation of deep water at present²⁹, must subsequently be lost by denitrification/anammox elsewhere, for example in the suboxic OMZs of the Indo-Pacific⁴. Much of the remaining global N₂ fixation seems to occur locally to these regions⁴, resulting in a rapid feedback with fixed-N loss^{1,3,4} and hence minimal impact on the global fixed-N inventory². In contrast, the non-local balance we suggest to result from interactions between the overturning circulation and Fe supply in the Atlantic (Figs 1–3), although representing only $\sim 10\text{--}15\%$ of global marine N₂ fixation estimated at present (Table 1), contributes to the potential for significant perturbations of the N inventory, as any feedback must operate on deep ocean circulation (100 s–1,000 yr) timescales^{2,5,8,9,15}.

In contrast to a strict close coupling between N inputs and losses⁴, a degree of spatial decoupling² is required if, for example, past changes in North Atlantic N₂ fixation reflected adjustment to altered rates of denitrification/anammox in remote OMZs (refs 15, 30). Iron control of N₂ fixation (Fig. 2), combined with large-scale transport of excess P (Fig. 3), may potentially contribute to such decoupling. Our results thus have important implications for understanding how the oceanic nitrogen inventory might respond to altered circulation^{15,27} or dust deposition patterns^{5,8,9}.

Methods

Near-surface measurements. Meridional gradients of surface layer (0–300 m) biological and chemical variables were measured during the AMT-17 cruise onboard the RRS *Discovery* from 15 October to 28 November 2005. Sea water was collected using trace-metal clean techniques with either a titanium conductivity–temperature–depth rosette frame fitted with trace-metal clean Niskin bottles or a towed fish and Teflon bellows pump system. Biological rate measurements and chemical analyses were carried out using standard protocols.

Hydrographic and nutrient data. Data used for examining deep-ocean N* (equivalent P*) distributions and calculating fluxes were taken from the Geochemical Ocean Section Study (GEOSECS) west Atlantic section and World Ocean Circulation Experiment (WOCE) lines A10, A17 and A20. Full methods and any associated references are included in the Supplementary Information.

Received 3 June 2009; accepted 28 September 2009;
published online 1 November 2009

References

1. Redfield, A. C. The biological control of chemical factors in the environment. *Am. Sci.* **46**, 205–221 (1958).
2. Codispoti, L. A. in *Productivity of the Ocean: Present and Past* (eds Berger, W., Smetacek, V. & Wafer, G.) 377–394 (Wiley, 1989).
3. Tyrrell, T. The relative influences of nitrogen and phosphorus on oceanic primary production. *Nature* **400**, 525–531 (1999).
4. Deutsch, C., Sarmiento, J. L., Sigman, D. M., Gruber, N. & Dunne, J. P. Spatial coupling of nitrogen inputs and losses in the ocean. *Nature* **445**, 163–167 (2007).
5. Falkowski, P. G. Evolution of the nitrogen cycle and its influence on the biological sequestration of CO₂ in the ocean. *Nature* **387**, 272–275 (1997).
6. Mills, M. M., Ridame, C., Davey, M., La Roche, J. & Geider, R. J. Iron and phosphorus co-limit nitrogen fixation in the eastern tropical North Atlantic. *Nature* **429**, 292–294 (2004).
7. Berman-Frank, I., Quigg, A., Finkel, Z. V., Irwin, A. J. & Haramaty, L. Nitrogen-fixation strategies and Fe requirements in cyanobacteria. *Limnol. Oceanogr.* **52**, 2260–2269 (2007).
8. Moore, J. K. & Doney, S. C. Iron availability limits the ocean nitrogen inventory stabilizing feedbacks between marine denitrification and nitrogen fixation. *Glob. Biogeochem. Cycles* **21**, GB20001 (2007).
9. Broecker, W. S. & Henderson, G. M. The sequence of events surrounding Termination II and their implications for the cause of glacial-interglacial CO₂ changes. *Paleoceanography* **13**, 352–364 (1998).

10. Li, Y. H. & Peng, T. H. Latitudinal change of remineralization ratios in the oceans and its implication for nutrient cycles. *Glob. Biogeochem. Cycles* **16**, 1130 (2002).
11. Gruber, N. & Sarmiento, J. L. Global patterns of marine nitrogen fixation and denitrification. *Glob. Biogeochem. Cycles* **11**, 235–266 (1997).
12. Wu, J., Sunda, W., Boyle, E. A. & Karl, D. M. Phosphate depletion in the Western North Atlantic Ocean. *Science* **289**, 759–762 (2000).
13. Hood, R. R., Coles, V. J. & Capone, D. G. Modeling the distribution of *Trichodesmium* and nitrogen fixation in the Atlantic Ocean. *J. Geophys. Res.* **109**, CO6006 (2004).
14. Capone, D. G. *et al.* Nitrogen fixation by *Trichodesmium* spp.: An important source of new nitrogen to the tropical and subtropical North Atlantic Ocean. *Glob. Biogeochem. Cycles* **19**, GB2024 (2005).
15. Galbraith, E. D., Kienast, M., Pedersen, T. F. & Calvert, S. E. Glacial–interglacial modulation of the marine nitrogen cycle by high-latitude O₂ supply to the global thermocline. *Paleoceanography* **19**, PA4007 (2004).
16. Mahaffey, C. *et al.* Biogeochemical signatures of nitrogen fixation in the eastern North Atlantic. *Geophys. Res. Lett.* **30**, 1300 (2003).
17. Tyrrell, T. *et al.* Large-scale latitudinal distribution of *Trichodesmium* spp. in the Atlantic Ocean. *J. Plankton Res.* **25**, 405–416 (2003).
18. Voss, M., Croot, P., Lochte, K., Mills, M. M. & Peeken, I. Patterns of nitrogen fixation along 10° N in the tropical North Atlantic. *Geophys. Res. Lett.* **31**, L23S09 (2004).
19. Sohm, J. A. & Capone, D. G. Phosphorus dynamics of the tropical and subtropical North Atlantic: *Trichodesmium* spp. versus bulk plankton. *Mar. Ecol. Progr. Ser.* **317**, 21–28 (2006).
20. Hansell, D. A., Olson, D. B., Dentener, F. & Zamora, L. M. Assessment of excess nitrate development in the subtropical North Atlantic. *Mar. Chem.* **106**, 562–579 (2007).
21. Moore, C. M. *et al.* Relative influence of nitrogen and phosphorus availability on phytoplankton physiology and productivity in the oligotrophic sub-tropical North Atlantic Ocean. *Limnol. Oceanogr.* **53**, 291–305 (2008).
22. Sanudo-Wilhelmy, S. A. *et al.* Phosphorus limitation of nitrogen fixation by *Trichodesmium* in the central Atlantic Ocean. *Nature* **411**, 66–69 (2001).
23. Yamamoto-Kawai, M., Carmack, E. & McLaughlin, F. Nitrogen balance and Arctic throughflow. *Nature* **443**, 43–43 (2006).
24. Sarmiento, J. L., Gruber, N., Brzezinski, M. A. & Dunne, J. P. High-latitude controls of thermocline nutrients and low latitude biological productivity. *Nature* **427**, 56–60 (2004).
25. Williams, R. G., Roussenov, V. & Follows, M. J. Nutrient streams and their induction into the mixed layer. *Glob. Biogeochem. Cycles* **20**, GB1016 (2006).
26. McDonagh, E. L. & King, B. A. Oceanic fluxes in the South Atlantic. *J. Phys. Oceanogr.* **35**, 109–122 (2005).
27. Rahmstorf, S. Ocean circulation and climate during the past 120,000 years. *Nature* **419**, 207–214 (2002).
28. Deutsch, C., Gruber, N., Key, R. M., Sarmiento, J. L. & Ganachaud, A. Denitrification and N₂ fixation in the Pacific Ocean. *Glob. Biogeochem. Cycles* **15**, 483–506 (2001).
29. Ganachaud, A. & Wunsch, C. Improved estimates of global ocean circulation, heat transport and mixing from hydrographic data. *Nature* **408**, 453–457 (2000).
30. Ren, H. *et al.* Foraminiferal isotope evidence of reduced nitrogen fixation in the ice age Atlantic Ocean. *Science* **323**, 244–248 (2009).

Acknowledgements

We thank the scientific complement and crew of the RRS *Discovery* during AMT-17 for all of their assistance. P. Holligan, A. Martin, R. Sanders and T. Tyrrell are thanked for discussions and comments on the manuscript. This work was supported by EU Carboocean grants to R.J.G. and J.L.R. and the UK Natural Environment Research Council, through a fellowship to C.M.M. and the Atlantic Meridional Transect consortium. This is contribution number 172 of the AMT programme.

Author contributions

R.J.G., J.L.R., C.M.M., M.M.M. and E.P.A. designed the research. C.M.M., M.M.M., E.P.A., M.I.L., X.P., D.J.S., S.J.U. and E.M.S.W. collected samples and carried out the work at sea. M.J.A.R. analysed iron samples. A.J.P. enumerated *Trichodesmium*. C.M.M. and E.L.M. analysed nutrient distributions and calculated transport data. C.M.M. wrote the first draft of the paper. C.M.M., M.M.M., R.J.G., J.L.R. and E.P.A. discussed the results and extensively edited subsequent drafts. All of the authors commented on the manuscript.

Additional information

Supplementary information accompanies this paper on www.nature.com/naturegeoscience. Reprints and permissions information is available online at <http://npg.nature.com/reprintsandpermissions>. Correspondence and requests for materials should be addressed to C.M.M.